

NEW MEASUREMENT TECHNIQUES FOR THE ON LINE DIMENSION CHARACTERIZATION OF AUTOMOTIVE RUBBER PROFILES

R. Anchini, G. Di Leo, C. Liguori, A. Paolillo

DIII University of Salerno, via Ponte don Melillo, Fisciano (SA), Italy – email: tliguori@unisa.it

Abstract: A vision-based measurement system for the online inspection of automotive rubber profiles is described. The system determines a 3-D reconstruction of the rubber profile section and performs dimensional measurements. After a brief description of the whole measurement system, the main novelties are pointed out: the simple calibration procedure and the flexible tools allowing users to specify the dimensional measurements regardless of the type of the profile to be inspected.

Keywords: Contact-less measurement, machine vision, automotive profile.

1. INTRODUCTION

The industry is today very attracted by the possibilities given by the inspection of products performed by image-based measurement systems. The motivations include increased cost effectiveness, higher operating speeds, reliability, consistency and objectivity, and improved record keeping. For some applications, automated inspection using machine vision has had already a relevant number of applications. This is not the case for the production of rubber profiles, due to the complexity of the production process and to the nature of the product.

Authors already realized an image-based measurement system for inspection tasks in a plant producing rubber profiles for the automotive industry [1]-[2]. A stereo vision system was designed to make the on-line contour extraction, the 3D reconstruction of the transversal section of “single-bulb” rubber profiles, and the measurement of the main dimensional parameters. However, since the contour tracking procedures and the dimensional measurement procedures were specific for each particular profile, new types of profile to be produced required new software procedures to be thought and implemented. Since today’s automotive market forces to introduce new models of cars, and then new models of rubber profiles, more and more frequently, a first step towards a solution of these issues was the design of an all-purpose contour extraction procedure which was not depending on the shape of the profile [3]. However a complete solution was not yet achieved since also the measurement procedure has to be not depending on profile shapes.

This paper describes a novel application for the inspection of rubber profiles, which implements the required complete solution, since it can be maintained up to date for

new models of profiles simply by maintaining a proper database of profiles.

In the following, after a brief recall of the overall structure of the measurement station, which has a structure basically similar to the the previous one, the stages of the application will be detailed, mainly stressing the novel ones, namely the calibration procedure, the registration of each observed profile onto a reference profile and the tools allowing users to specify the dimensional measurements to be extracted from the different profiles. The proposed measurement system is currently operating on the production lines of a plant of the Metzeler Automotive Profile Systems group.

2. SYSTEM OVERVIEW

A constraint in the design of the measurement system was that it must not require any significant alteration of the production line structure and operation. Thus, it was located at the end of the line, near the conveyor belt bench (Fig. 1). It is provided with two cameras each one yielding a 2D image of the leading transversal section of the profile at the end of the extrusion process, but each one with a different perspective angle. Since the surface of profiles is dark and poorly reflecting, an illuminator lights up the profile section in order to increase image contrast. A photoelectric cell detects the presence of a profile in front of the cameras thus triggering the image acquisition and processing via an acquisition board held in an expansion slot of the elaboration unit (PC). During the image acquisition, that lasts about 500 ms, the profile must be kept still. To this aim a programmable delay circuit switches off the conveyor belt engine, while an upstream storage unit accumulates the product drawn in the meantime.

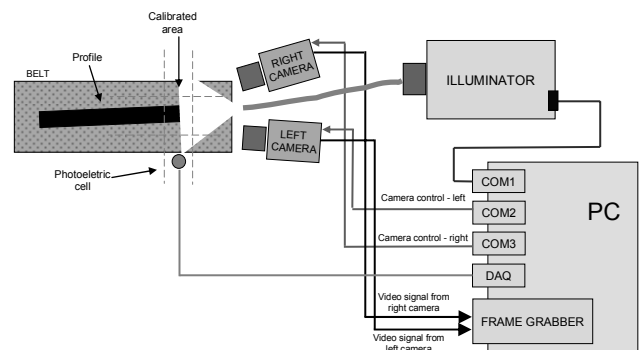


Fig. 1. The hardware architecture of the measurement station.

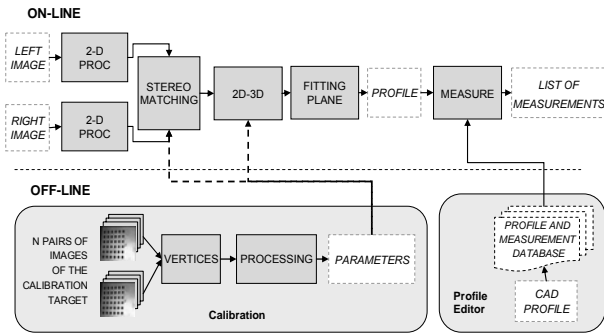


Fig. 2. The software architecture of the application.

The software architecture of the measurement station can be outlined in three main modules (Fig. 2). The first one, the “on-line” processing procedure, is run each time a new profile falls within the field of view of the two cameras. The two acquired images undergo the same 2-D processing steps (histogram enhancement, contour extraction performed through region growing [4]) up to the sampling of the points belonging to left and right 2-D contours. Subsequent on-line processing steps determine 3-D point coordinates and extract the final measurements requested by the user.

The on-line module needs data that are determined off-line by other modules: the calibration parameters and the database of the profiles. The former ones are obtained at the end of the calibration procedure, that will be detailed in Section 3, and are used by the algorithms that determine the 3-D representation of the contour. The profile and measurement database is an archive containing all the profiles and the geometrical definitions of the dimensions to be measured. This archive is upgradeable by the user through a specific software module of the developed application, called the “Profile Editor”.

3. CALIBRATION

The purpose of the calibration is to establish the relationship between 3-D world coordinates expressed in the so-called world frame (a coordinate system having arbitrary position and orientation in the space, which final measurements have to be referred to) and their corresponding 2-D image coordinates in the so-called image frame (the 2-D coordinate system defined on the camera sensor plane, which pixel locations in the image can be referred to) as seen by the computer. Once this relationship is established, 3-D information can be inferred from 2-D information and vice versa. The equation describing the mapping between the 3D coordinates M of a scene point and the coordinates of its projection m onto the image plane is expressed as: $\lambda m = PM$, where λ is an unknown scale factor, P is called the projection matrix and depends on the unknown camera parameters.

In stereo-vision imaging systems, an additional step to be faced up is the determination of the relative position of both cameras, represented through the transformation necessary to move the reference system integral with the first camera to the reference system integral with the second camera. It can be showed that if a world point has

respectively X_L and X_R as vectors of coordinates in the coordinate systems associated to the first and the second camera, the transformation is written as follows:

$$X_R = RX_L + T$$

where R and T are the rotation and the translation matrices defining the transformation. A calibration session gives as results the matrices R and T describing the relative position of the both cameras and the projection matrices P_L and P_R . Given the coordinates of two image points m_l and m_r , projections of the same 3-D scene point M , the 3-D point is imaged in the left and right view as:

$$\lambda_L m_L = P_L M \text{ and } \lambda_R m_R = P_R M \quad (1)$$

If the world reference frame is fixed onto the left camera:

$$P_L = K_L [I | 0] \text{ and } P_R = K_R [R | T], \quad (2)$$

where K_L and K_R depend on the intrinsic parameters (camera constant, principal point, distortion factors) of the left and right camera respectively. Eventually, the 3-D coordinates of M can be found by solving eq. (1) [10].

An *ad hoc* calibration algorithm has been developed starting from the well-known procedure proposed by Zhang [5], which requires the two cameras to observe a planar target, whose geometry in 3-D space is known with very good precision, shown at a few different orientations (at least five). The target can be freely moved and the motion needs not be known. A sandblasted metal plate (see Fig. 3) containing a pattern of 6x5 square holes (120 squares corners) is adopted as the target, instead of the commonly adopted paper sheet printings [5], due to its better accuracy ($\sim 10 \mu m$). The knowledge of the corner positions in several pairs of images, at least five, and of the target geometry in millimetres allow specific calculations based on the maximum likelihood criterion [5] in order to determine the parameters of the vision system.

A procedure for the corner detection in calibration images has been implemented, which yields two pairs of 2-D image coordinates for each target corner. A preliminary coarse estimation of corner positions is obtained through a semiautomatic procedure that requires the user to click on the four extreme corners of the pattern in each acquired image. All the vertices of the square holes are estimated at first approximately with a linear interpolation. This initial estimation is refined by a template matching technique. Four templates representing ideal corners are used, one for each



Fig. 3: Target corner detection during the calibration.

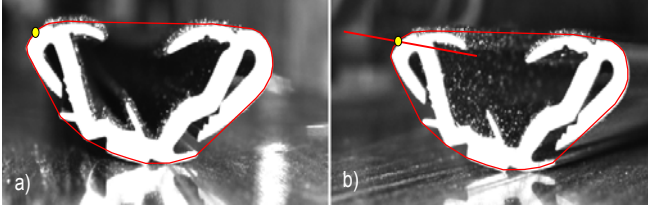


Fig. 4: Examples of convex hulls of (a) left and (b) right images. Also two corresponding points and a piece of right epipolar line are reported.

possible corner orientation to be detected in the image. The adopted technique consists of moving a template w on an image area around the early estimated position of the corner and computing the normalized cross-correlation C in that area. The maximum value of C indicates the position where w best matches the image. A screenshot of the final corner detection is reported in Fig. 3.

3. THE 3-D RECONSTRUCTION

As can be seen in Fig. 2, the on-line section of the 3-D reconstruction phase can be divided into two stages: i) the search for matching stereo pairs (*i.e.* the pair of images in left and right images corresponding to the same real point), and ii) the determination of the actual 3-D coordinates of each point of the profile contour as a function of the two stereo pairs. Both stages require the knowledge of calibration parameters, determined during the off-line calibration phase. The search for stereo pairs exhibits several difficulties in the case of rubber profiles, since the possible shapes of rubber profiles are extremely changeable and thus no *a priori* hypothesis can be made about the geometrical curve describing the profile. The proposed algorithm exploits the generally valid epipolar constraint [6]: basically, given a point image on one image (*e.g.* the left one), the corresponding point on the other (*e.g.* the right) image lies on a line, the so-called epipolar line, whose localization can be determined from the calibration parameters. The point on the right image which corresponds to a given point on the left image can be searched for within the intersections between its epipolar line and the profile contours.

However, due to the possible complex shapes of the section profiles, the actual matching point of the pair can not be discriminated reliably with the criteria known in literature. For this reason, matching stereo pairs are located on the contours of the convex hulls of the profiles in the two images at first. The convex hull of a 2-D set of points is the smallest convex polygon that includes the points. The advantage of the introduction of the convex hull is that there are always only two intersections between an epipolar line and the contour of a convex hull. An example is reported in Fig. 4, where a point is considered on left 2-D convex hull (Fig. 4(a)), and its corresponding right epipolar line is plotted on right image (Fig. 4(b)); the intersection between the epipolar segment and the right 2-D convex hull is taken as the point on right image corresponding to the considered point on left image. The 3-D coordinates of the points of the convex hull of the 3-D profile can be easily determined with the procedure proposed in [5]. The hypothesis that a 3-D

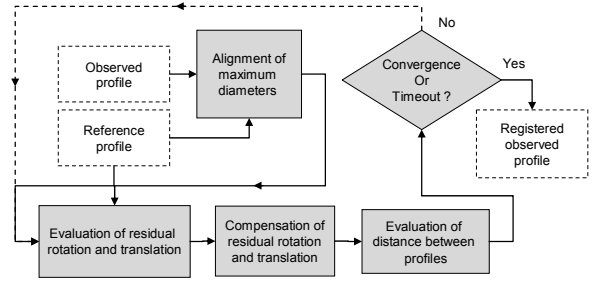


Fig. 5: Block diagram of the registration algorithm.

reconstruction of the convex hull of a profile lies on the same plane of the profile itself allows to state that the transformation which moves the left-image convex hull onto the 3-D convex hull is the same transformation which moves the left profile onto the 3-D profile. Then the parameters of this transformation (a linear roto-translation with rescaling of coordinates) are estimated with a fitting algorithm. Eventually, this transformation is applied to each point of the left-image contours in order to achieve the 3-D representation of the whole profile. In order to simplify the subsequent extraction of measurements from the profile, the best fitting plane where the 3-D profile lies is determined and the 2-D projection of the profile on this plane is evaluated and considered for the measurement phase.

4. THE MEASUREMENTS ON PROFILES

In order to fulfill to the requirements of the quality monitoring of rubber profiles, the following issues have been considered and included in the software: i) the observed profile of each profile piece has to be superimposed (“registered”) onto the reference profile for that kind of profile, for comparison purposes; this result has been accomplished with an *ad hoc* developed roto-translation function which minimizes the distance between profiles; ii) the set of dimensions to be measured is specified separately for each profile; in this case, a user-friendly software interface lets the user to define measurement segments locked to the reference profile; iii) the measurements of the dimensions are compared with design tolerance limits and a “pass/fail” result has to be displayed.

4.1 The registration of profiles

The need for an on-line inspection of profiles has influenced the choice of the registration algorithm, since solutions available in literature, such as the Iterative Closest Point (ICP) algorithm [7], require a relevant elaboration time. A registration algorithm has been developed in order to have quite an accurate but approximate registration with a limited elaboration time. The block diagram of the registration algorithm is reported in Fig. 5. At first, the segment connecting the two farthest points of the profile (the “maximum diameter”) is determined for each one of the two input profiles, and the observed profile is roto-translated as long as its maximum diameter coincides with the maximum diameter of the reference profile (in orientation and middle point). The criterion adopted for the evaluation of the goodness of the registration is the minimization of the average of the distances of closest point pairs, *i.e.* composed of a point of a profile and of a point of the other profile

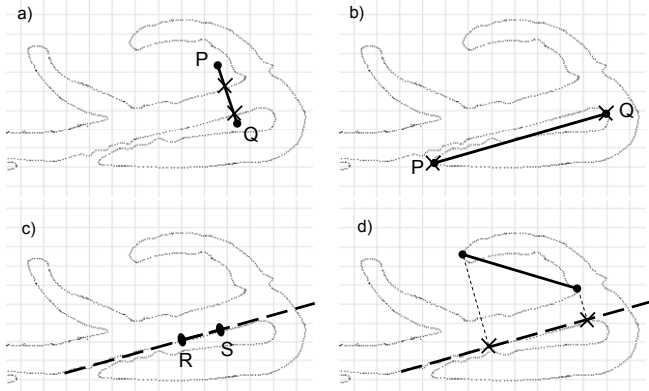


Fig. 6: Measurement tools applied to a profile: a) “gauge”; b) “tip-to-tip”; c) axis definition; d) “tip-to-tip” projected on an axis (the extremes of measured lengths are marked with “x” in all cases).

which is closest to the former one. If the vector distances, \underline{d}_i , between two closest points are considered, the translation to be compensated can be estimated as the vector average of the \underline{d}_i . In order to estimate the residual rotation, the relationship between the average of normalized vector products $(\underline{d}_i \times \underline{r}_i)/L$ and the residual rotation angle has been empirically evaluated, where \underline{r}_i is the vector radius connecting the i^{th} point and the middle point of the maximum diameter, and L is the length of the maximum diameter. After a refinement of position and angle, the distance between the two profiles, defined as the average of the distance between closest points, is evaluated and compared to the value of the required target distance. If the actual profile distance is lower than the target profile, or a timeout interval is not elapsed, a new step of rototranslation compensation is executed, otherwise the procedure stops.

Achieved execution times of the whole registration procedure are of the order of some seconds for final average distances of the order of tenth of mm.

4.2 The measurements on profiles

The segments to be measured on the profile depend on the specific type of profile. A specific software tool, the “Profile Editor”, can be used by operators or profile designers in order to define the set of measurement for each type of profile. A set of basic measurement tools has been defined that can be placed on a reference profile design (example are shown in Fig. 6). After an observed profile is registered onto the reference profile, the segment defined by the specified tool within the coordinate system of the reference profile is measured on the observed profile. Three types of measurement tool have been introduced:

- “Gauge”: a segment is specified and the distance

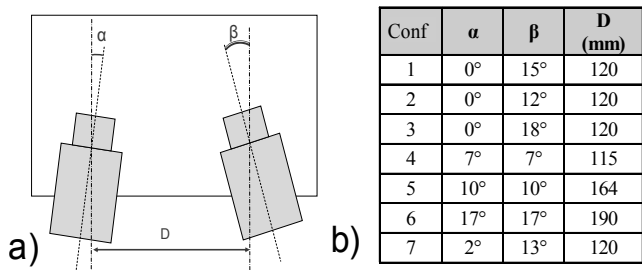


Fig. 7: Camera orientation: a) definition of parameters; b) values adopted in the tests.

between the two intersections of the segment and the observed profile is returned.

- “Axis”: a line is identified by searching for the two points of the observed profile which are closest to the specified ones.

- “Tip-to-tip”: the corner points which are closest to those specified are considered on the observed profile, and their distance is returned. This measurement can be also projected on a previously specified axis.

Eventually, the user interface of the on-line module displays, for each piece: the two profiles, the table of last results, the time chart of the results and some statistics.

5. THE EXPERIMENTAL CHARACTERIZATION

With the objective of carrying out the metrological characterization of the measurement system, a set of tests were performed in order to evaluate, (i) the influence of the relative position of the cameras, (ii) the systematic error of the measurement system and (iii) the repeatability of the measurement results.

Some reference objects have been used during the tests. For each reference object, a set of contours of the nominal section has been accurately edited by CAD operators, in order to be used as reference profile during the registration and measurement phase of the software application.

The experimental characterization was carried out on the system in use at Metzeler APS Factory in Battipaglia, Italy.

5.1 Evaluation of sensitivity to camera orientation

A set of multiple measurements have been carried out with different relative positions of the cameras in order to evaluate the sensitivity of measurement results to the orientations of the two cameras. The adopted cameras have a 1/2” CCD sensor and the focal length of the optics is 25mm.

The angles of camera axis and the baseline are defined in Fig. 7(a); the values reported in Fig. 7(b) have been adopted for the tests.

For each camera configuration, the following tests have been carried out: 20 executions of the on-line processing procedure for each one of the 5 different positions of the object in the calibration volume (centre, left, right, centre-right and centre-left). For each object, 4 geometrical measurements have been defined. This set of measurements have been repeated for 4 reference objects: 3 metallic gauge blocks (15x15 mm, 15x30 mm and 30x30 mm) and a metallic bar with the same cross-section of a profile. The gauge blocks have been used since they are widely adopted as standard references in mechanical measurements (less

Tab. I: Mean and standard deviation of results obtained in the seven considered geometrical configurations.

Conf	E mean	E max	σ
1	0.037	1.438	0.339
2	-0.240	1.311	0.502
3	-0.028	1.341	0.346
4	0.048	0.946	0.310
5	0.146	1.410	0.345
6	0.296	2.333	0.712
7	-0.162	0.655	0.279

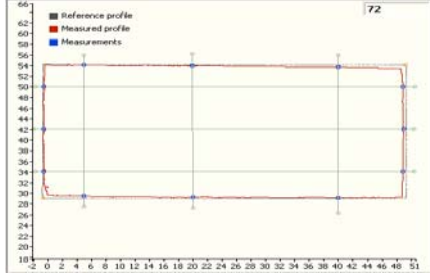


Fig. 8: Measurement results on gauge blocks.

than 1 μm accuracy), while the metallic profile has been adopted since it can be measured both by the proposed system as an ordinary rubber profile and by an accurate contact measurement system, thus allowing a comparison of the results achieved by the image-based measurement system in operating conditions with more accurate measurements.

An overall number of 1600 (4 geometrical quantities \times 20 repetitions \times 5 position \times 4 objects) measurements for each camera orientation have been made. Tab. I shows the mean value, the maximum value and the standard deviations of the errors for each camera configuration (Conf).

As you can see from the results of Tab. I, the configuration n° 7 is been characterized by the lowest maximum error and standard deviation, as a consequence this configuration is used in the proposed measurement system.

5.2 Systematic errors

In order to determine possible systematic effects, repeated measurements have been carried out on the 25x50 mm metallic gauge block. In particular, the object was placed in three different positions of the calibration area, and for each position the on-line processing procedure was run 20 times. The system is configured in order to perform three measurements of height and three measurements of width (see Fig. 8) obtaining an overall number of 180 horizontal and 180 vertical geometrical measurements. On these results a statistical analysis is carried out in order to estimate systematic errors and consequently calculate the correction factors.

The horizontal and vertical correction factors, C_W and C_H respectively, are calculated using the nominal values, W_n

Tab. II: The results of the evaluation of correction factors.

Horizontal				
W_{meas}	W_n	$\sigma_{W_{meas}}$	C_W	u_{C_W}
49.35 mm	50.00 mm	0.08 mm	1.013	0.002
Vertical				
H_{meas}	H_n	$\sigma_{H_{meas}}$	C_H	u_{C_H}
24.57 mm	25.00 mm	0.03 mm	1.017	0.002

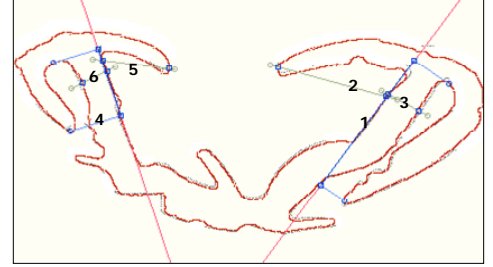


Fig. 9: Measurement results on the reference metallic profile.

and H_n , and the measured average values along the two directions, respectively W_{meas} and H_{meas} :

$$C_H = \frac{H_n}{H_{meas}}; \quad C_W = \frac{W_n}{W_{meas}} \quad (3)$$

The uncertainties of correction factors are evaluated as in relationship (4):

$$u_{C_H} = C_H \frac{\sigma_{H_{meas}}}{H_{meas}}; \quad u_{C_W} = C_W \frac{\sigma_{W_{meas}}}{W_{meas}} \quad (4)$$

where σ_* stands for the standard deviation of the mean of the corresponding quantity. The achieved correction factors, showed in Tab.II, have been stored in a file and are loaded and applied by the measurement procedure during the normal operation.

5.3 Evaluation of the repeatability

In order to evaluate the repeatability of the proposed measurement system, two kinds of experimental measurements have been carried out using different reference objects: (i) a metallic object with the same shape of a specific rubber profile (see Fig.9), and (ii) two rubber profiles.

(i) After 6 different measurements (depicted in Fig. 9) had been defined for the metallic profile in the profile editor, it

Tab. III: Results for the metallic object in 10 different positions.

Nominal Value	(1) 15.0 mm		(2) 10.5 mm		(3) 3.2 mm		(4) 6.9 mm		(5) 6.3 mm		(6) 2.6 mm	
	μ	σ	μ	σ	μ	σ	μ	σ	μ	σ	μ	σ
Pos. 1	0.27	0.05	0.15	0.03	0.04	0.04	0.27	0.03	0.10	0.06	0.00	0.05
2	0.20	0.07	0.15	0.07	0.03	0.06	0.23	0.07	0.12	0.07	-0.01	0.05
3	0.20	0.08	0.08	0.05	-0.09	0.04	0.25	0.07	0.09	0.05	-0.11	0.05
4	-0.03	0.09	0.20	0.03	0.30	0.02	0.03	0.07	0.26	0.06	-0.01	0.03
5	0.20	0.05	0.17	0.07	-0.03	0.04	0.24	0.03	0.17	0.05	0.08	0.06
6	0.03	0.11	0.06	0.06	0.07	0.03	0.18	0.11	0.07	0.06	-0.07	0.03
7	-0.12	0.03	0.21	0.02	0.23	0.02	-0.11	0.00	0.23	0.10	-0.04	0.02
8	0.12	0.08	0.16	0.05	0.00	0.03	0.01	0.06	0.13	0.05	0.06	0.03
9	0.19	0.03	0.06	0.06	0.04	0.04	0.17	0.06	0.10	0.02	0.08	0.05
10	0.19	0.02	0.10	0.04	0.06	0.02	0.19	0.04	0.17	0.05	-0.03	0.06

Tab IV: Results of repeatability evaluation (measurements in mm).

QL	μ AS	σ AS	QL	μ AS	σ AS
8.3	8.34	0.20	10.5	10.39	0.18
2.4	2.53	0.12	3.2	3.13	0.17
6.5	6.45	0.26	6.3	6.21	0.15
9.0	9.00	0.12	2.6	2.58	0.10
10.0	10.08	0.22	15.0	14.75	0.15
15.1	15.22	0.17	6.9	6.73	0.17

was manually placed in ten different positions within the calibration area, and, for each position, the on-line processing procedure was run 20 times. Tab. III summarizes the results of these tests in terms of mean and standard deviation of the errors for each geometrical measurement. Very low residual systematic effects are observed. Since these effects depend on object position and on the measurand itself, they can not be corrected. Moreover, taking into account the residual error and measurement standard deviation, it is possible to state that all the provided results are characterized by an uncertainty equal or less than 0.2 mm.

(ii) In order to verify the metrological characteristics in typical operating conditions, another set of tests have been carried out. Two different rubber profiles have been positioned repeatedly on the conveyor belt for 50 times each, and the on-line processing procedure has been run each time. In Figs. 10(a) and 10(b), the screenshots for the two profiles are reported. In Tab. IV, the results for the two objects are summarized. The table reports, for comparison purposes, also measurements obtained in the quality laboratory (“QL” column) with the ordinary procedure (a sliced sample of profile is put on a 10X magnifier lens and the geometrical values are obtained on the slice projection), which have an uncertainty (about 0.3 mm) greater than the one of the proposed automatic measurement system. All the measurement values obtained with the two methods are compatible (see Tab. IV). As for the measurement repeatability, a maximum standard deviation equal to 0.26 mm is measured, thus confirming the previous results (uncertainty equal to 0.2 mm for each measurement values).

CONCLUSIONS

A stereovision-based measurement system for the online inspection of automotive rubber profiles has been presented, which performs dimensional measurements on the profile of transversal sections of rubber extrusions. The main algorithms adopted in the application have been detailed, and the results of the metrological characterization carried out in the actual operating environment have been reported and discussed. The proposed system is currently operating on the production lines in a Metzeler APS plant. The achieved performances (overall uncertainty of the provided dimensional measurements within 0.2 mm) meet the requirements of the quality inspection of such rubber products.

REFERENCES

- [1] L. Angrisani, P. Daponte, A. Pietrosanto, C. Liguori. “An image based measurement system for the characterization of automotive gaskets”. *Measurement* 25 (1999) 169-181.
- [2] C. Liguori, A. Paolillo, A. Pietrosanto. “An on-line stereovision system for dimensional measurement of rubber extrusions”. *Measurement* 35 (2004) 221-231
- [3] C. Liguori, A. Paolillo, A. Pietrosanto. “On-line automatic selection of measurement procedures for dimensional rubber gasket characterisation”. 12th IMEKO TC4, Zagreb, Croatia, vol.II, pp.390-395, 2002
- [4] R.C.Gonzalez, R.E.Woods. “Digital Image Processing”. 2nd Ed., Prentice Hall, 2002. ISBN: 0-201-18075-8.
- [5] Z. Zhang. “A Flexible New Technique for Camera Calibration”. Microsoft Research Technical Report, MSR-TR-98-71, 2002.
- [6] R. Jain, R. Kasturi, B. G. Schunck. “Machine Vision”. McGraw-Hill Science.
- [7] Z. Zhang. “Iterative point matching for registration of free-form curves and surfaces”. *International Journal of Computer Vision*, 13:119-152, 1994.
- [8] “Handbook of image & video processing”, Editor AI Bovik, Academic Press, 2st edition, 2005
- [9] B. Girod, G. Greiner, H. Niemann. “Principles of 3D image Analysis and Synthesis”, Kluwer Academic Publishers.
- [10] O. Faugeras, “Three-Dimensional Computer Vision”, MIT Press, 1993.

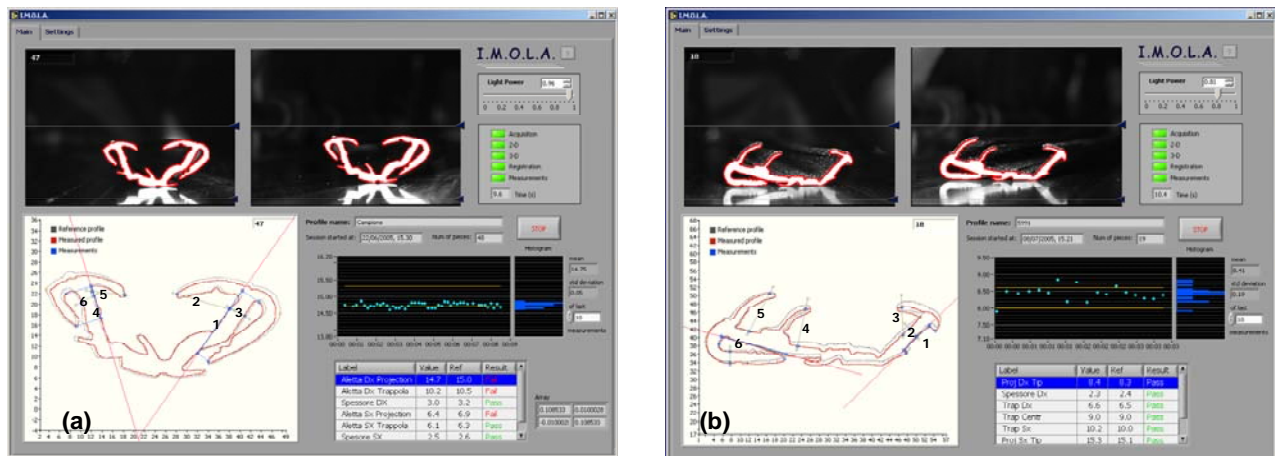


Fig. 10: Screenshots of the system output.